The face of Glut1-DS patients: a 3D craniofacial morphometric analysis.

Valentina Pucciarelli[1], Simona Bertoli[2], Marina Codari[3], Ramona De Amicis[2], Valentina De Giorgis[4], Alberto Battezzati[2], Pierangelo Veggiotti[4,5] and Chiarella Sforza[1].

[1]LAFAS, Laboratorio di Anatomia Funzionale dell'Apparato Stomatognatico Dipartimento di Scienze Biomediche per la Salute Università degli Studi di Milano, Italy

[2] Dipartimento di Scienze per gli Alimenti, la Nutrizione e l'Ambiente, Università degli Studi di Milano, Milano, Italy;

[3]Unit of Radiology, IRCCS Policlinico San Donato, Via Morandi 30, San Donato Milanese, 20097, Milan, Italy

[4]Dept. Child Neurology and Psychiatry, C. Mondino National Neurological Institute, Pavia, Italy

[5]Brain and Behaviour Department, University of Pavia, Pavia, Italy

Submitted to Clinical Anatomy on April 9th, 2017

Presented in abstract form at the 1° European Conference on Glut1 DS (Milan, Italy), 2016

Running title: The face of Glut1-DS patients

Number of Tables 4

Number of Figures 5

Conflict of interest

The authors declare they have no competing interests.

Corresponding author:
Prof. Chiarella Sforza
Department of Biomedical Sciences for Health
Università degli Studi di Milano
via Mangiagalli 31
20133 Milano
Italy.
Phone: +39 0250315407
Fax: +39 0250315387
e-mail: chiarella.sforza@unimi.it

This article has been accepted for publication and undergone full peer review but has not been through the copyediting, typesetting, pagination and proofreading process which may lead to differences between this version and the Version of Record. Please cite this article as an 'Accepted Article', doi: 10.1002/ca.22890

The face of Glut1-DS patients: a 3D craniofacial morphometric analysis

Abstract

Introduction - Glut1 deficiency syndrome (Glut1-DS) is a neurological and metabolic disorder caused by impaired transport of glucose across the blood brain barrier (BBB). Mutations on the SCL2A1 gene encoding the glucose transporter protein in the BBB cause the syndrome, which encompasses epilepsy, movement disorders and mental delay. Such variability of symptoms presents an obstacle to early diagnosis. The patients seem to share some craniofacial features, and identification and quantification of these could help in prompt diagnosis and clinical management.

Materials and method - We performed a three-dimensional morphometric analysis of the faces of 11 female Glut1-DS patients using a stereophotogrammetric system. Data were analyzed using both inter-landmark distances and Principal Component Analysis (PCA).

Results - Compared to data collected from age-, sex- and ethnicity-matched control subjects, common and homogenous facial features were identified among patients, which were mainly located in the mandible and the eyes. Glut1-DS patients had a more anterior chin; their mandibular body was longer but the rami were shorter, with a reduced gonial angle; they had smaller and down-slanted eyes with a reduced intercanthal distance.

Conclusions - This study highlights the importance of morphometric analysis for defining the facial anatomical characteristics of the syndrome better, potentially helping clinicians to diagnose Glut1-DS. Imnproved knowledge of the facial anatomy of these patients can provide insights into their facial and cerebral embryological development, perhaps further clarifying the molecular basis of the syndrome.

Key words: Glut1 deficiency syndrome; stereophotogrammetry; face; principal component analysis

Introduction

Described in 1991 as an epileptic encephalopathy with an early childhood onset, Glut1 deficiency syndrome (Glut1-DS, OMIM #606777; ORPHA:21772) is a neurological and metabolic disorder caused by impaired transport of glucose across the blood brain barrier (BBB) (De Vivo et al., 1991; Brockmann et al., 2001; Klepper, 2015; De Giorgis et al., 2016).

Despite the earlier classification of the disease as "classical" and "non-classical", depending on the type of epileptic seizures and other associated features, Glut1-DS is now considered a spectrum encompassing different conditions such as epilepsy, movement disorders, ataxia, dystonia, spasticity, speech problems, delayed mental development, and other paroxysmal events (Brockmann et al., 2001; De Giorgis et al., 2015; Leen et al., 2010). Isolated cases of hemolytic anemia and cryohydrocytosis have also been described, but they are not currently included in the clinical picture, which nevertheless could also be completed by acquired microcephaly and prognathism (Weber et al., 2008; Flatt et al., 2017; Fe 2008; Valentina De Giorgis et al., 2015).

Glucose is the main fuel for the human brain, but being hydrophilic it needs a transporter to cross the hydrophobic BBB and the other tissues in order to be used as an energy source (Todor, 2016). Mutations on the gene SCL2A1 (1p35-31.3), which encodes glucose transporter type 1, lead to impaired glucose transport into the brain and cause the syndrome (De Vivo et al., 2002). They can arise *de novo* or be transmitted in an autosomal dominant manner, although some sporadic cases have been described (De Giorgis et al., 2015; Klepper et al., 2003).

Impaired glucose transport to the brain leads to reduced levels of glucose in the cerebral spinal fluid (CSF) in the presence of normal glycemia. For this reason, diagnosis of this syndrome is currently based on lumbar puncture, which permits the cerebral glucose levels to be measured. This can be

followed by mutational analysis of the gene SCL2A1. More than 100 mutations have been associated with deletion or loss of function of the transporter protein, causing an insufficient cerebral glucose supply (Klepper, 2015; Leen et al., 2010; Nakken et al., 2013).

To date, this condition has been treated using a ketogenic diet (Lepper et al., 2002; Voit, 2004). Ketones provide an alternative fuel for the brain when glucose type 1 transporters are not available, and the ketogenic diet showed good results in terms of reducing epileptic seizures and paroxysm (De Giorgis and Veggiotti, 2013). These observations led Schoeler et al. to question whether a positive response to such a dietetic plan among patients affected by generalized epilepsy, but with negative genetic testing, could be associated with undiagnosed Glut1-DS (Schoeler et al., 2015). For example, a recent Japanese study showed that in a group of 32 patients, 12.5% had those features (Ito et al., 2015).

Since the symptoms associated with this condition are variable, diagnosis is usually challenging (Diomedi et al., 2016). Clinical observations include craniofacial alterations such as microcephaly (Voit, 2004) and prognathism. In particular, a recent clinical report on Italian Glut1-DS patients found prognathism in 18% of the subjects analyzed, a Gestalt sign of the disease that was confirmed by a pilot morphometric study (De Giorgis et al., 2015; Pucciarelli et al., 2015).

Indeed, different syndromes are characterized by a typical facial phenotype that can guide clinicians towards the diagnosis (Pucciarelli et al., 2015), and quantitative three-dimensional (3D) facial assessments can better define phenotypical subgroups or highlight features that can be lost in a simple clinical inspection (Hammond et al., 2013; Inglese et al., 2016; Pucciarelli et al., 2016; Hurren and Flack, 2016; Sachdeva et al., 2016).

The use of optical, contact-less instruments such as stereophotogrammetry or laser scans has greatly improved and facilitated craniofacial quantification. These instruments are non-invasive, easy to use

and fast, making them suitable for the 3D acquisition of facial images from syndromic patients, even in cases of more or less serious mental delay, as in Glut1-DS patients (Sforza et al., 2013).

The aim of this study is to perform a 3D stereophotogrammetric assessment of the Glut1-DS facial phenotype in order to quantify facial shape and size variations through multivariate statistical techniques (De Giorgis et al., 2015; Goodwin et al., 2014; Hennekam 2005; Dolci et al., 2016).

Materials and Methods

This study was performed according to the tenets of the Declaration of Helsinki and after approval by the ethics committee of UniversitàdegliStudi di Milano, 27 June 2014, no.266 230 92/2014. Before data acquisition, each subject or the parents/legal guardians read and signed an informed consent. Verbal consent was also obtained from all subjects. None of the procedures was invasive or dangerous and all were performed with minimal discomfort for the subjects.

In total, 216 subjects were analyzed: 11 females, aged 3-32 years, with genetically ascertained diagnosis of Glut1-DS, and 205 control subjects. The control subjects were selected to be paired for age and sex to the Glut1-DS patients. Each reference group comprised a minimum of 13 subjects. All subjects were Caucasian and had no previous history of facial trauma or surgery. The patients included one mother/daughter pair, while the rest were unrelated. Table 1 gives details of the mutations identified in the patient group.

Facial images of the patients and reference subjects were acquired using a stereophotogrammetric system (VECTRA M3, Canfield Scientific Inc. Fairfield, NJ, USA), an optical instrument that captures facial images simultaneously from different points of view and merges them to generate a 3D surface facial reconstruction. The system is fast, non-invasive and suitable for subjects who are not completely cooperative (Sforza et al., 2013). Before the acquisitions, the faces of the patients and control subjects were marked with a set of 42 anthropometric landmarks using a black liquid eye-liner. Landmarks were identified by an expert operator through gentle palpation or visual inspection, using a standardized procedure (Ferrario et al., 2003). All subjects were asked to maintain a neutral facial expression during the acquisition, with lips and teeth in loose contact. An example of stereophotogrammetric reconstruction of the face of a young patient is shown in figure

1, where the landmarks examined are indicated by their acronyms. A detailed description of the landmarks used has been published (Ferrario et al., 2003).

After the 3D facial reconstruction, the landmarks of interest were identified and digitized on the facial surfaces and their x, y, and z coordinates were extracted. These coordinates were used, together with those obtained from the reference subjects, to perform two different analyses: the calculation of landmark-to-landmark anthropometric distances, ratios, angles and areas (and their corresponding z-scores), and a Principal Components Analysis (PCA).

Anthropometric measurements

A series of linear distances, angles, areas, and ratios was calculated for both the patients and control subjects, starting from their three-dimensional coordinates (Table 2). Details of the measurements used were published previously (Sforza and Ferrario, 2006; Sforza et al., 2009). The measured values for the patients were transformed into z-scores using, for each measurement, the corresponding means and standard deviations of the reference group (Leiser et al., 2017). The average z-scores of the patients were subsequently compared with those of the controls using an unpaired Student's t test. The criterion for statistical significance was $p<0.05$.

Principal Components Analysis

In order to compare the facial morphologies of the Glut1-DS and control subjects, a PCA shape analysis was performed using Matlab (Mathworks, Natick, USA). To quantify the facial differences between the two groups, all the point clouds composed by the 42 analyzed anatomical landmarks were spatially superimposed using the procrustes registration method, which allows the translational, rotational and isometric scaling components to be adjusted optimally.

Once registered, the point clouds were used as input for a PCA, a multivariate approach that allows morphological variations within a face sample to be analyzed. In particular, PCA enables data dimensionality to be reduced, calculating a series of derived variables called principal components (PCs), which are linear combinations of the original variables and describe the axes of shape variation (Zelditch et al., 2012).

After the PC calculations, stepwise regression was used as a systematic method to identify a subset of predictors, in our case PCs, of the morphological differences between the faces of Glut1-DS and control subjects. The PCs included in the regression model were then assessed to identify the specific facial morphology of Glut1-DS subjects. The criterion for statistical significance was set at $p<0.05$.

Results

Anthropometric measurements

Table 3 shows the mean z-scores, their standard deviations (SD) and the corresponding p-values for the anthropometric measurements in the current study. Figures 2 and 3 are graphical representations of the statistically significant z-scores of the patients, arranged by anatomical region.

The distinctive characteristics of the patients' faces were mainly located in the eye and mandibular regions. In particular, patients had closer, smaller and more down-slanted eyes than control subjects because of the shorter intercanthal distance, ocular width in both right and left eyes, and soft-tissue ocular area. The deviation of the eye fissure from true horizontal was also less than control values on both sides.

Other features distinguishing Glut1-DS patients from controls were located in the middle and lower third of the face (maxilla and mandible). Both the middle and lower parts of the face were lower in patients; the difference from controls was greatest in the mandibular area. In contrast, their mandibular body was longer than in controls, with a lower sn-t/ pg-go ratio and a shorter mandibular ramus. Consequently, the ratio between the posterior and anterior facial heights was lower in patients. Furthermore, the patients had greater mandibular convexity, less convex lower faces, and more facial divergence than control subjects. Their gonial angles were smaller than those of the controls.

Principal components analysis

The analyzed sample included 216 point clouds (205 control and 11 Glut1-DS subjects) composed of 42 anatomical landmarks, defined in the 3D space. After PCA analysis, 126 PCs were calculated.

The first 22 of these allowed 90% of face variability within the sample to be described, while the first 71 described 99% of it.

Among the calculated PCs, only 23 were retained after stepwise regression. Table 3 shows the coefficient values and the corresponding p-values for these 23. Finally, to establish how these components affected facial morphology, we selected the three most significant: PC1, PC2, and PC9. Figure 4 shows how these three PCs affected facial morphology in the analyzed sample.

In the 3D space defined by PC1, PC2 and PC9, Glut1-DS patients all clustered in the negative parts of the three dimensions, with a more homogeneous distribution than control subjects (Figure 5). PC1 explained 44% of the total variance. The main variations were seen in the upper and lower parts of the face. Glut1-DS patients (average configuration minus **[should this be ±?]** 1.96 SD, Figure 4a) were characterized by a high forehead, smaller eyes and a prominent nose, a short mandibular ramus with a long mandibular body, small gonial angles, and a less prominent chin.

PC2 explained 9% of the total variance, and again depicted Glut1-DS patients with a high forehead, smaller eyes, and low chin prominence (average configuration minus **[should this be ±?]** 1.96 SD, Figure 4b). Also, the face was less deep and more divergent.

Modifications included in PC9 (2% of total variance) were focused in the oral region, Glut1-DS patients being characterized by more prominent lips and a less prominent chin (average configuration minus **[should this be ±?]** 1.96 SD, Figure 4c).

Discussion

Clinical manifestations of Glut1-DS are heterogeneous so it is not always easy to diagnose the condition. Indeed, the diagnosis can be very challenging, as in cases of familiar epilepsies with cognitive and motor function impairment (Diomedi et al., 2016). Nevertheless, early recognition of the syndrome could be very advantageous, facilitating correct treatment and prompt introduction of the ketogenic diet, which should be started as soon as possible and maintained at least until adolescence (Akman et al., 2016).

Despite the clinical variability of this syndrome, previous qualitative observations, corroborated by clinical practice, identified a typical facial aspect of the patients, with a tendency to a more prominent mandible and a retrognathic maxilla, as confirmed by a pilot morphometric study (De Giorgis et al., 2015; Pucciarelli et al., 2015). Such results underlined the need for the more detailed morphometric analysis performed in the current study, which again revealed a common set of craniofacial features among Glut1-DS patients.

Two morphometric techniques were used: a set of conventional anthropometric measurements, and PCA. Both offer benefits (Sforza et al., 2013): z-scores are widely used clinically, for example in fetal ultrasonography and to predict the presence of chromosomal aberrations (Chitkara et al., 2002); PCA is a strong statistical method that allows the main components of variability in spatial data to be identified. It has already been applied to morphometric analysis of the face, and it has been suggested as a future instrument for early recognition of the syndromes (Demšar et al., 2017; Goodwin et al., 2014). Moreover, morphometric analysis has already been proposed as a valid instrument to address other syndromes that have wide clinical manifestations or require early diagnosis (Dolci et al. 2016; Goodwin et al., 2014).

In general, the results of the conventional anthropometric measurements were confirmed and extended by the PCA, revealing a more homogeneous face in patients than controls, most of the

anomalies being located on the forehead (increased), eyes (decreased), nose (prominent), middle and lower facial width and depth (decreased), and the mandible. In particular, Glut1-DS patients seem to possess a long mandibular body with a short ramus and small gonial angles, reduced chin prominence and increased lip prominence, and increased facial divergence. It has to be mentioned that the facial configurations shown in Figure 4 do not necessarily represent actual faces; they are mathematical tools that allow the major characteristics of the patients to be highlighted.

The determination of precise facial features shared among Glut1-DS patients could be important for increasing understanding of the pathology and of its cellular and molecular bases. Jensen et al. demonstrated that abrogation of the *glut1* orthologue in zebra fish leads to impaired cerebral organogenesis, restored by expression of the human transporter mRNA (Jensen et al., 2006). Even if this experimental model is not ideally suited to describing exactly what happens in patients, since humans maintain a functional copy of the transporter, it is important to remember that, embryologically, the face and the brain are interlinked (Pucciarelli et al., 2016; Petryk et al., 2015). Therefore, alterations in brain development due to underlying genetic mechanisms and occurring at any level could be reflected in abnormal facial features (Sperber, 2001). Studies dedicated to clarifying these aspects are mandatory. For instance, the modifications seen in the upper part of the face of the current group of Glut1-DS patients (increased forehead and reduced soft-tissue eye dimensions) could somehow be related to altered brain development, as found macroscopically in forebrain pathologies such as holoprosencephaly (Pucciarelli et al., 2016).

The alterations seen in the mandibular area corroborated the clinical picture of prognathism described for these patients. Recent studies on subjects with mandibular prognathism, in most cases candidates for orthognathic surgery, revealed a set of genes related to the excess mandibular prominence. The locations of some of these genes on chromosome 1 (1p36; 1p22.3; 1p22.1;

1q32.2) seem to be adjacent to those identified as the basis of disease in Glut1-DS patients (1p35-31.3), possibly explaining the association between the two disorders by genetic linkage (Ikuno et al. 2014; Tassopoulou-Fishell et al., 2013; Chen et al. 2015).

Facial morphometric analysis, however elaborated, will obviously never replace clinical diagnosis coupled with recognized biochemical and genetic tests, but, given its safety and low cost, it can serve as an initial screening test or a valid supplement to genetic testing. It could also be used effectively for longitudinal assessments.

Knowledge of the specific facial morphology of the patients, aside from its anatomical importance, is a good starting point for predicting, planning, and evaluating the outcome of orthodontic and orthopedic treatments for patients. Indeed, facial scans are widely used in orthodontic assessment, because of the benefits provided from the 3D technology, but also because of the deeper anatomical characterization achievable through morphometric analysis (Kau et al., 2010).

Conclusion

The present study highlighted the importance of recognizing typical and common facial features among Glut1-DS patients through a non-invasive, 3D, morphometric approach. This will open the way to morphometric analysis of the face as an ancillary tool for early diagnosis of this syndrome and other medical conditions in which a more or less evident facial dysmorphism can be involved.

Considering the limited number of patients in this study, and the fact that they were all female, it will be mandatory to increase the sample size and to investigate the facial features of male patients too.

REFERENCES

Akman CI, Yu J, Alter A, Engelstad K, De Vivo DC. 2016, Diagnosing Glucose Transporter 1 Deficiency at Initial Presentation Facilitates Early Treatment. J Pediatr, 171, 220-6.

Arsov, T. 2016, GLUT-1 deficiency: From pathophysilogy and genetics to abroad clinical spectrum. Sanamed, 11, 151-155.

Bhuiyan ZA, Klein M, Hammond P, van Haeringen A, Mannens MM, Van Berckelaer-Onnes I, Hennekam RC. 2006, Genotype-phenotype correlations of 39 patients with Cornelia De Lange syndrome: the Dutch experience. J Med Genet, 43, 568-75.

Brockmann K, Wang D, Korenke CG, von Moers A, Ho YY, Pascual JM, Kuang K, Yang H, Ma L, Kranz-Eble P, Fischbarg J, Hanefeld F, De Vivo DC. 2001, Autosomal dominant glut-1 deficiency syndrome and familial epilepsy. Ann Neurol, 50, 476-85.

Chen F, Li Q, Gu M, Li X, Yu J, Zhang YB. 2015, Identification of a Mutation in FGF23 Involved in Mandibular Prognathism. Sci Rep, 10, 11250.

Chitkara U, Lee L, Oehlert JW, Bloch DA, Holbrook RH Jr, El-Sayed YY, Druzin ML. 2002, Fetal ear length measurement: a useful predictor of aneuploidy? Ultrasound Obstet Gynecol, 19, 131-5.

De Giorgis V, Varesio C, Baldassari C, Piazza E, Olivotto S, Macasaet J, Balottin U, Veggiotti P. 2016, Atypical Manifestations in Glut1 Deficiency Syndrome. J Child Neurol, 31, 1174-80.

De Giorgis V, Veggiotti P. 2013, GLUT1 deficiency syndrome 2013: current state of the art. Seizure, 22, 03-11.

De Giorgis V, Teutonico F, Cereda C, Balottin U, Bianchi M, Giordano L, Olivotto S, Ragona F, Tagliabue A, Zorzi G, Nardocci N, Veggiotti P. 2015, Sporadic and familial glut1ds Italian patients: A wide clinical variability. Seizure, 24, 28-32.

De Menezes M, Rosati R, Ferrario VF, Sforza C. 2010, Accuracy and reproducibility of a 3 dimensional stereophotogrammetric imaging system. J Oral Maxillofac Surg, 2010, 68, 2129-35.

De Vivo DC, Leary L, Wang D. 2002, Glucose transporter 1 deficiency syndrome and other glycolytic defects. J Child Neurol, 17, S15-23.

De Vivo DC, Trifiletti RR, Jacobson RI, Ronen GM, Behmand RA, Harik SI. 1991, Defective glucose transport across the blood-brain barrier as a cause of persistent hypoglycorrhachia, seizures, and developmental delay. N Engl J Med, 325,703-9.

Demšar U, Harris P, Brunsdon C, Fotheringham AS, McLoone S. 2013, Principal Component Analysis on Spatial Data : An Overview Principal Component Analysis on Spatial Data. Ann AssAm Geogr, 103, 106-28.

Diomedi M, Gan-Or Z, Placidi F, Dion PA, Szuto A, Bengala M, Rouleau GA, Gigli GL. 2016, A 23 years follow-up study identifies GLUT1 deficiency syndrome initially diagnosed as complicated hereditary spastic paraplegia. Eur J Med Genet, 59, 564-568.

Dolci C, Pucciarelli V, Codari M, Marelli S, trifirò G, pini A. 2016, 3D Morphometric Evaluation of Craniofacial Features in Adult Subjects with Marfan Syndrome. Proc 7th Int Conf 3D Body Scanning Technol Lugano, Switzerland, 98–104.

Ferrario VF, Sforza C, Serrao G, Ciusa V, Dellavia C. 2003, Growth and aging of facial soft tissues: A computerized three-dimensional mesh diagram analysis. Clin Anat, 16, 420-33.

Flatt JF, Guizouarn H, Burton NM, Borgese F, Tomlinson RJ, Forsyth RJ, Baldwin SA, Levinson BE, Quittet P, Aguilar-Martinez P, Delaunay J, Stewart GW, Bruce LJ. 2011, Stomatin-deficient cryohydrocytosis results from mutations in SLC2A1: a novel form of GLUT1 deficiency syndrome. Blood, 10, 118, 5267-77.

Giuca MR, Inglese R, Caruso S, Gatto R, Marzo G, Pasini M. 2016, Craniofacial morphology in

pediatric patients with Prader-Willi syndrome: a retrospective study. Orthod Craniofac Res, 19, 216-221.

Goodwin AF, Larson JR, Jones KB, Liberton DK, Landan M, Wang Z, Boekelheide A, Langham M, Mushegyan V, Oberoi S, Brao R, Wen T, Johnson R, Huttner K, Grange DK, Spritz RA, Hallgrímsson B, Jheon AH, Klein OD, 2014. Craniofacial morphometric analysis of individuals with X-linked hypohidrotic ectodermal dysplasia. Mol Genet Genomic Med, 2, 422-9.

Hammond P, Suttie M, Hennekam RC, Allanson J, Shore EM, Kaplan FS. 2012, The face signature of fibrodysplasia ossificans progressiva. Am J Med Genet A, 158A, 1368-80.

Hurren BJ, Flack NA. Prader-Willi Syndrome: A spectrum of anatomical and clinical features. 2016, Clin Anat, 29, 90-605.

Ikuno K, Kajii TS, Oka A, Inoko H, Ishikawa H, Iida J. 2014, Microsatellite genome-wide association study for mandibular prognathism. Am J Orthod Dentofacial Orthop, 145, 757-62.

Ito Y, Takahashi S, Kagitani-Shimono K, Natsume J, Yanagihara K, Fujii T, Oguni H. 2015, Nationwide survey of glucose transporter-1 deficiency syndrome (GLUT-1DS) in Japan. Brain Dev, 37, 780-9.

Jensen PJ, Gitlin JD, Carayannopoulos MO. 2006, GLUT1 deficiency links nutrient availability and apoptosis during embryonic development. J Biol Chem, 281, 13382-7.

Kau CH, Richmond S, Zhurov A, Ovsenik M, Tawfik W, Borbely P, English JD. 2010, Use of 3-dimensional surface acquisition to study facial morphology in 5 populations. Am J Orthod Dentofacial Orthop, 137, S56.e1-9.

Klepper J. 2015, GLUT1 deficiency syndrome and ketogenic diet therapies: missing rare but treatable diseases? Dev Med Child Neurol, 57, 896-7.

Klepper J, Diefenbach S, Kohlschütter A, Voit T. 2004, Effects of the ketogenic diet in the glucose transporter 1 deficiency syndrome. Prostaglandins Leukot Essent Fatty Acids, 70, 321-7.

Klepper J, Flörcken A, Fischbarg J, Voit T. 2003, Effects of anticonvulsants on GLUT1-mediated glucose transport in GLUT1 deficiency syndrome in vitro. Eur JPediatr, 162, 84-9.

Klepper J, Leiendecker B, Bredahl R, Athanassopoulos S, Heinen F, Gertsen E, Flörcken A, Metz A, Voit T. 2002 Introduction of a ketogenic diet in young infants. J Inherit Metab Dis, 25, 449-60.

Leen WG, Klepper J, Verbeek MM, Leferink M, Hofste T, van Engelen BG, Wevers RA, Arthur T, Bahi-Buisson N, Ballhausen D, Bekhof J, van Bogaert P, Carrilho I, Chabrol B, Champion MP, Coldwell J, Clayton P, Donner E, Evangeliou A, Ebinger F, Farrell K, Forsyth RJ, de Goede CG, Gross S, Grunewald S, Holthausen H, Jayawant S, Lachlan K, Laugel V, Leppig K, Lim MJ, Mancini G, Marina AD, Martorell L, McMenamin J, Meuwissen ME, Mundy H, Nilsson NO, Panzer A, Poll-The BT, Rauscher C, Rouselle CM, Sandvig I, Scheffner T, Sheridan E, Simpson N, Sykora P, Tomlinson R, Trounce J, Webb D, Weschke B, Scheffer H, Willemsen MA. 2010, Glucose transporter-1 deficiency syndrome: the expanding clinical and genetic spectrum of a treatable disorder. Brain, 133, 655-70.

Leiser Y, Barak M, Ghantous Y, Yehudai N, Abu El-Naaj I. 2017, Indications for Elective Tracheostomy in Reconstructive Surgery in Patients With Oral Cancer. J Craniofac Surg, 28, e18-e22.

OMIM, http://omim.org/entry/606777, accessed March 2017.

ORPHANET, http://www.orpha.net/consor/cgi-bin/OC_Exp.php?Lng=IT&Expert=71277, accessed March 2017.

Petryk A, Graf D, Marcucio R. 2015, Holoprosencephaly: signaling interactions between the brain and the face, the environment and the genes, and the phenotypic variability in animal models and humans. Wiley Interdiscip Rev Dev Biol, 4, 17-32.

Pucciarelli V, Bertoli S, Codari M, Veggiotti P, Battezzati A, Sforza C. 2017, Facial Evaluation in Holoprosencephaly. J Craniofac Surg, 28, e22-e28.

Pucciarelli V, Codari M, Invernizzi C, Bertoli S, Battezzati A, De Amicis R, De Giorgis V, Veggiotti P, Sforza C. 2015, Three-Dimensional Craniofacial Features of Glut1 Deficiency Syndrome Patients. Proc 6th Int Conf 3D Body Scanning Technol Lugano, Switzerland.

Ramm-Pettersen A, Nakken KO, Skogseid IM, Randby H, Skei EB, Bindoff LA, Selmer KK. 2013, Good outcome in patients with early dietary treatment of GLUT-1 deficiency syndrome: results from a retrospective Norwegian study. Dev Med Child Neurol, 55, 440-7.

Sachdeva R, Donkers SJ, Kim SY. 2016, Angelman syndrome: A review highlighting musculoskeletal and anatomical aberrations. Clin Anat, 29, 561–7.

Schoeler NE, Cross JH, Drury S, Lench N, McMahon JM, MacKay MT, Scheffer IE, Sander JW, Sisodiya SM. 2015, Favourable response to ketogenic dietary therapies: undiagnosed glucose 1 transporter deficiency syndrome is only one factor. Dev Med Child Neurol, 57, 969-76.

Sforza C, De Menezes M, Ferrario V. 2013, Soft- and hard-tissue facial anthropometry in three dimensions: what's new. J Anthropol Sci, 91, 159-84.

Sforza C, Ferrario VF. 2006, Soft-tissue facial anthropometry in three dimensions: from anatomical landmarks to digital morphology in research, clinics and forensic anthropology. J Anthr Sci, 84:97–124.

Sforza C, Grandi G, Pisoni L, Di Blasio C, Gandolfini M, Ferrario VF. 2009, Soft tissue facial morphometry in subjects with Moebius syndrome. Eur J Oral Sci, 117, 695-703.

Sperber GH. 2001, Early orofacial development. In: Sperber GH, ed. Craniofacial Development. Hamilton: BC Decker Inc; 31–48.

Tassopoulou-Fishell M, Deeley K, Harvey EM, Sciote J, Vieira AR. 2012, Genetic variation in myosin 1H contributes to mandibular prognathism. Am J Orthod Dentofacial Orthop, 141, 51-9.

Weber YG, Storch A, Wuttke TV, Brockmann K, Kempfle J, Maljevic S, Margari L, Kamm C, Schneider SA, Huber SM, Pekrun A, Roebling R, Seebohm G, Koka S, Lang C, Kraft E, Blazevic D, Salvo-Vargas A, Fauler M, Mottaghy FM, Münchau A, Edwards MJ, Presicci A, Margari F, Gasser T, Lang F, Bhatia KP, Lehmann-Horn F, Lerche H.2008, GLUT1 mutations are a cause of paroxysmal exertion-induced dyskinesias and induce hemolytic anemia by a cation leak. J Clin Invest, 118, 2157-68.

Zelditch ML, DL Swiderski H, Sheets D, Fink WL. 2012, Geometric morphometrics for biologists: a primer.

Zorzi G, Castellotti B, Zibordi F, Gellera C, Nardocci N. 2008, Paroxysmal movement disorders in GLUT1 deficiency syndrome. Neurology, 71, 146-8.

Figure legends

Figure 1. Anthropometric landmarks identified on a patient's face. Acronyms indicate the reference points actually used in this study.

Figure 2. Statistically significant z-scores of the eye region (mean ± 1 SD). The continuous line indicates the reference z-score of the controls, which by definition is 0.

Figure 3. Statistically significant z-scores of the mandibular region (mean ± 1 SD). The continuous line indicates the reference z-score of the controls, which by definition is 0.

Figure 4 a, b, c. Effect of the variation of the three most significant PCs included in the regression model. For each PC, the average configuration, and those differing ± 1.96 SD, are depicted.

Figure 5. Comparison of Glut1-DS and control subjects in the principal component space, defined by the three more significant components included in the regression model. The ellipse highlights how the Glut1-DS subjects are distributed.

Table 1. Glut1-DS patients involved in the study and their mutations. Patients #1 and 2 are related

Patient#	sex	Age (years)	Protein Mutation	Type of mutation
1	female	11	V165I	missense
2	female	32	V165I	missense
3	female	29	R126C	missense
4	female	14	p.Thr295Met /pT295M9	missense
5	female	27	W48X	nonsense
6	female	18	c.457C>T	missense
7	female	8	p.N34S	missense
8	female	3	R249Afs131X	nonsense
9	female	17	p.Arg 400 cys	missense
10	female	8	p.Leu124TrpfsX12	deletion
11	female	10	R153C	missense

Table 2. Anthropometric measurements performed in this study

Distances [mm]		**Angles [°]**	
Intercanthal distance	ex-ex	Sagittal convexity (excluding nose)	n-sn-pg
Middle facial width	t-t	Sagittal facial convexity (including nose)	n-prn-pg
Lower facial width	go-go	Midfacial to mandibular plane	(t-n)-(pg-go)
Ocular width (right and left)	en-ex	Inclination of the eye fissure versus the true horizontal	en-ex^THR
Mouth width	ch-ch	Maxillary prominence	sl-n-sn
Forehead height	tr-n	Mandibular convexity	go-pg-go
Height of the nose	n-sn	Gonial angle (right and left)	t-go-pg
Lower facial height	sn-pg	Lower facial convexity	t-pg-t
Total facial height	n-pg		
Upper facial depth	n-t		
Middle facial depth	sn-t		
Lower facial depth	pg-t		
Mandibular corpus length	pg-go		
Mandibluar ramus length	t-go		
Width of the face	zy-zy		
Areas [cm^2]		**Ratios [%]**	
Soft-tissue ocular area (right and left)		Facial width/ total facial height ratio	t-t/n-pg
		Middle/lower facial depth ratio	sn-t/pg-t
		Middle facial depth/ mandibular corpus length ratio	sn-t/pg-go
		Posterior/anterior facial height ratio	t-go/sn-pg

Table 3. Mean, standard deviations (SD) and p-values of the anthropometric measurements performed

		Mean	SD	p-value			Mean	SD	p-value
Distances [mm]	ex-ex	-1.712	1.013	< 0.01	Angles [°]	n-sn-pg	-0.694	0.646	< 0.01
	t-t	-0.633	0.939	0.05		n-prn-pg	-0.224	0.544	0.201
	go-go	0.360	0.803	0.168		(t-n)-(pg-go)	1.143	0.856	< 0.01
	en-ex	-1.407	0.777	< 0.01		en-ex^THR	-1.453	0.801	< 0.01
	en-ex	-1.291	0.721	< 0.01		en-ex^THR	-0.984	0.740	< 0.01
	ch-ch	-0.506	1.427	0.267		sl-n-sn	0.483	0.798	0.072
	tr-n	-0.129	1.651	0.801		go-pg-go	-1.300	0.479	< 0.01
	n-sn	0.686	1.156	0.077		t-go-pg	-1.439	0.878	< 0.01
	sn-pg	0.186	1.591	0.707		t-pg-t	1.372	0.968	< 0.01
	n-pg	0.478	0.907	0.111					
	n-t	-0.650	0.941	0.045	Ratios [%]	t-t/n-pg	-0.822	0.923	0.014
	sn-t	-1.333	0.969	< 0.01		sn-t/pg-t	1.376	0.909	< 0.01
	pg-t	-1.986	1.096	< 0.01		sn-t/pg-go	-1.427	1.485	0.01
	pg-go	1.225	0.764	< 0.01		t-go/sn-pg	-1.522	1.103	< 0.01
	t-go	-1.764	0.945	< 0.01	Areas [cm^2]	Soft-tissue ocular area right	-1.019	0.477	< 0.01
	zy-zy	-0.649	1.242	0.113		Soft-tissue ocular area left	-1.063	0.564	< 0.01

Table 4. Coefficient values of the PCs included in the regression model and the corresponding t and p-values

	Coefficients	t-value	p-value
PC 1	-0.002	-5.921	$1.5 \cdot 10^{-8}$
PC 2	-0.005	-7.277	$8.5 \cdot 10^{-12}$
PC 3	-0.002	-2.635	$9.1 \cdot 10^{-3}$
PC 6	0.006	5.150	$6.4 \cdot 10^{-7}$
PC 9	-0.009	-5.695	$4.6 \cdot 10^{-8}$
PC 11	0.004	2.532	0.012
PC 13	-0.006	-2.876	0.005
PC 14	-0.005	-2.595	0.012
PC 21	-0.011	-4.062	$7.1 \cdot 10^{-5}$
PC 22	0.008	2.856	0.005
PC 23	-0.007	-2.208	0.028
PC 34	-0.009	-2.234	0.027
PC 36	-0.016	-3.637	$3.5 \cdot 10^{-4}$
PC 41	-0.013	-2.539	0.012
PC 47	-0.012	-2.004	0.046
PC 59	-0.018	-2.383	0.018
PC 66	0.019	2.117	0.036
PC 71	0.026	2.606	0.009
PC 86	-0.039	-2.754	0.007
PC 95	-0.055	-3.027	0.003
PC 100	0.051	2.430	0.016
PC 113	-0.105	-2.856	0.005

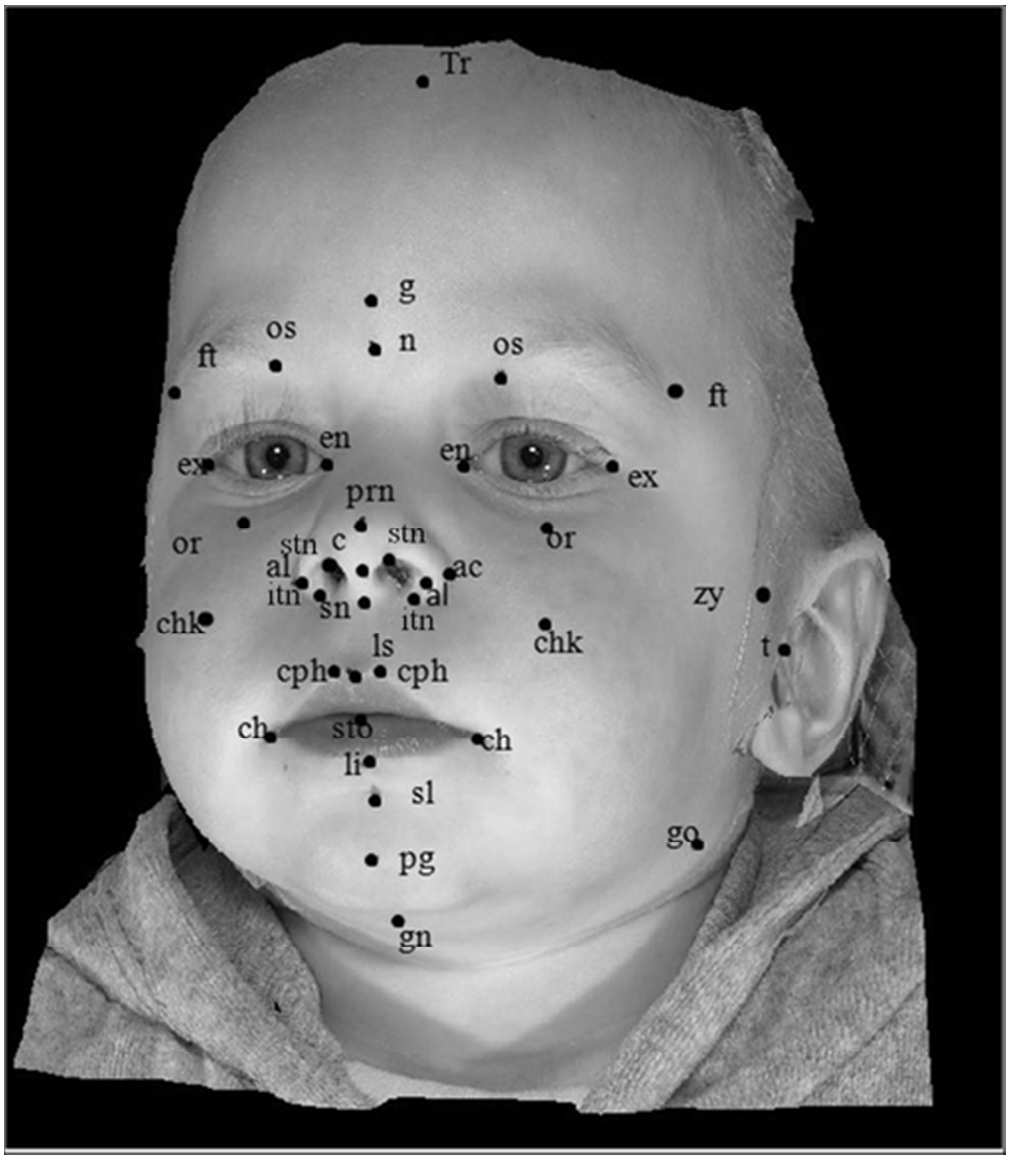

Figure 1. Anthropometric landmarks identified on a patient's face. Acronyms indicate the reference points actually used in this study.

42x49mm (300 x 300 DPI)

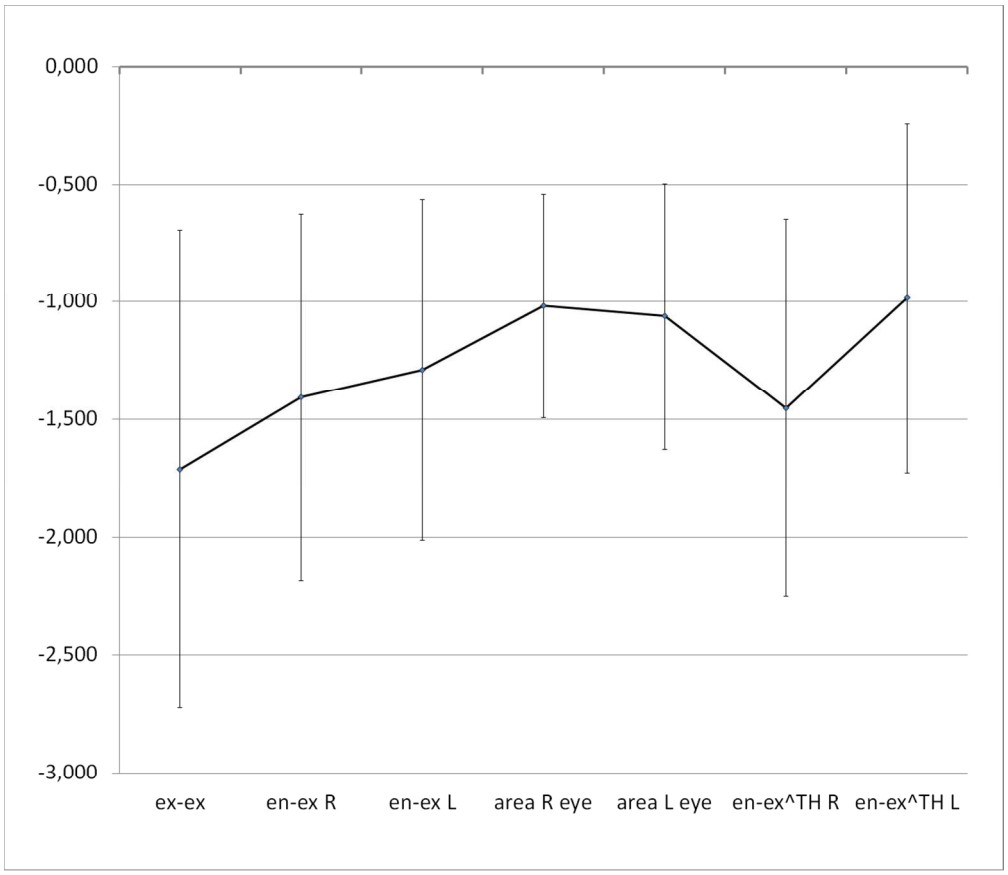

Statistically significant z-score values of the eye region (mean ± 1 SD). Continuous line indicates the reference z-score of the controls, that by definition is 0.

485x419mm (72 x 72 DPI)

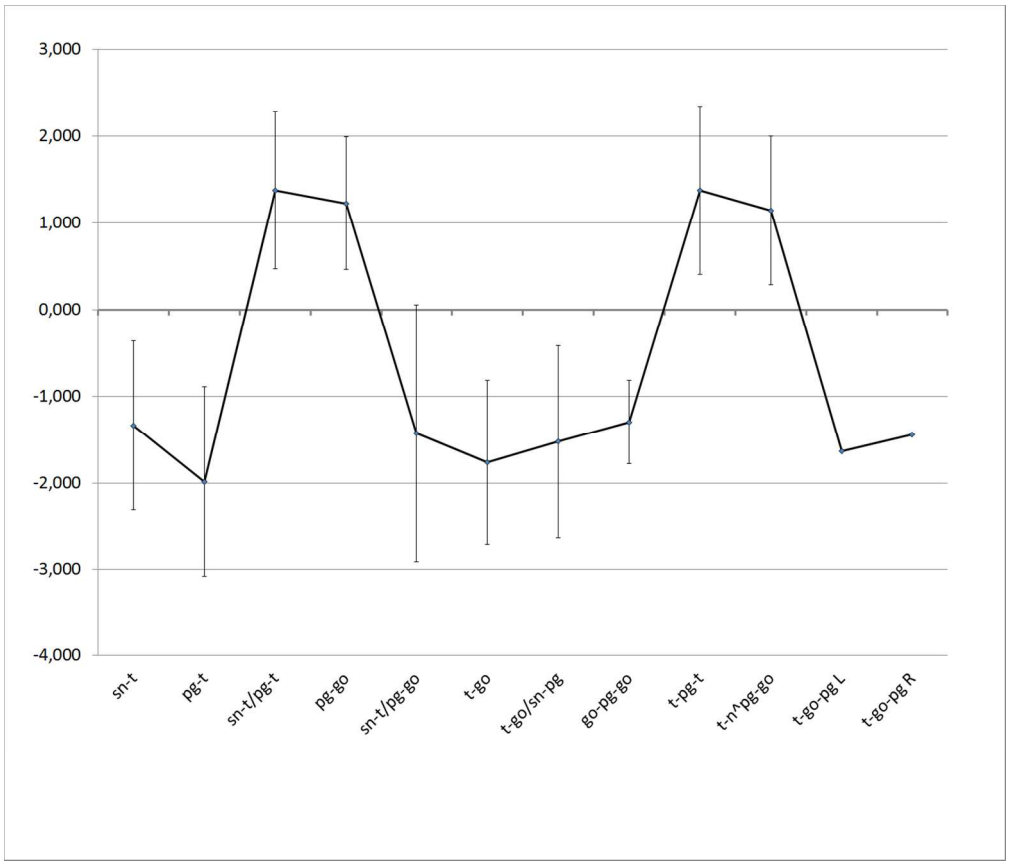

Statistically significant z-scores values of the mandibular region (mean ± 1 SD). Continuous line indicates the reference z-score of the controls, that by definition is 0.

508x434mm (72 x 72 DPI)

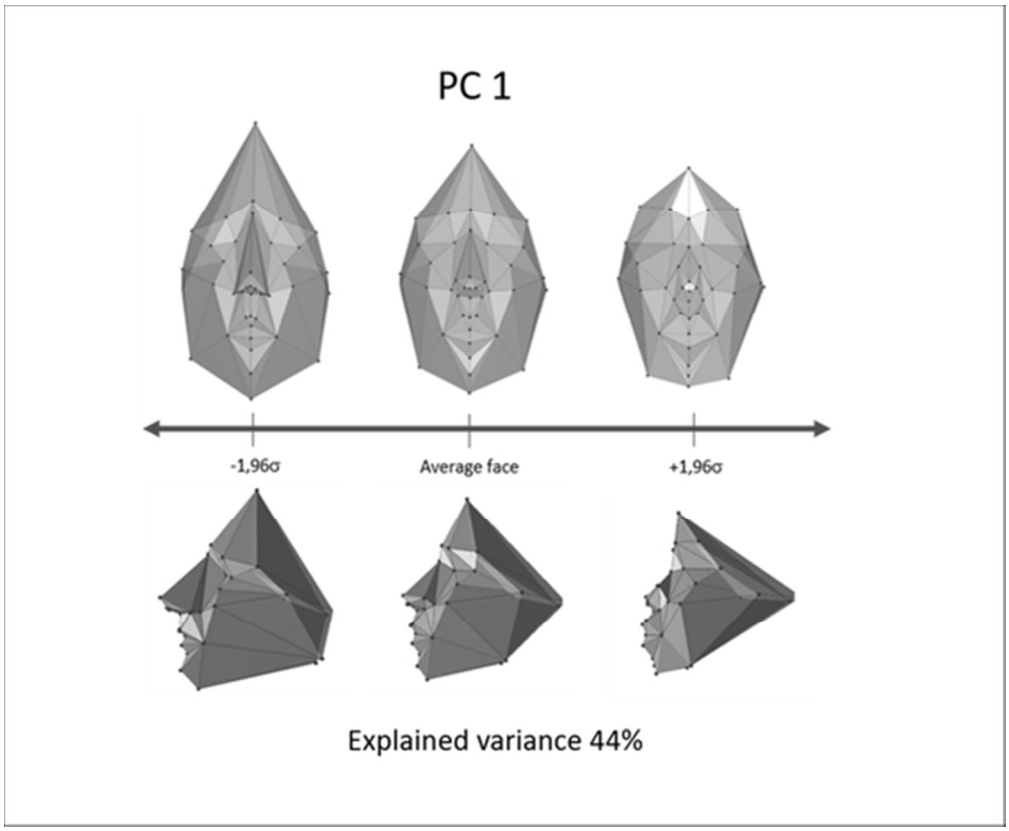

Effect of the variation of the three most significant PCs included in the regression model. For each PC, the average configuration, and those differing ± 1.96 SD, are depicted.

47x39mm (300 x 300 DPI)

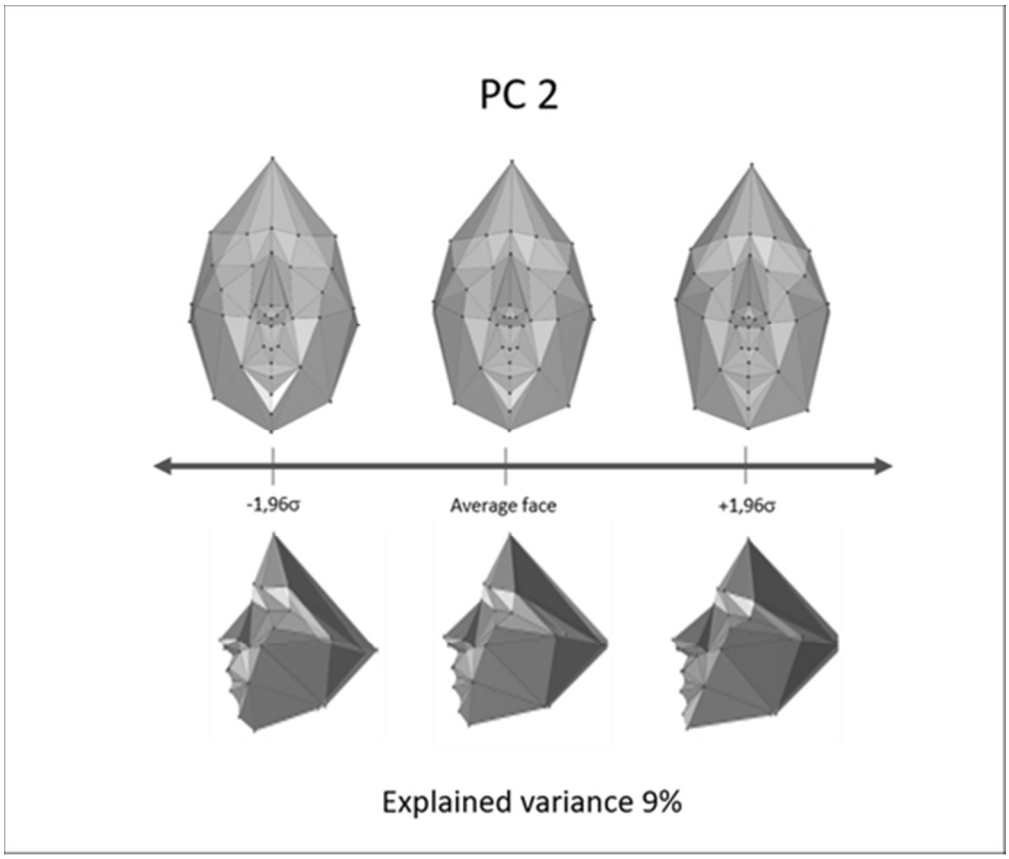

Effect of the variation of the three most significant PCs included in the regression model. For each PC, the average configuration, and those differing ± 1.96 SD, are depicted.

45x38mm (300 x 300 DPI)

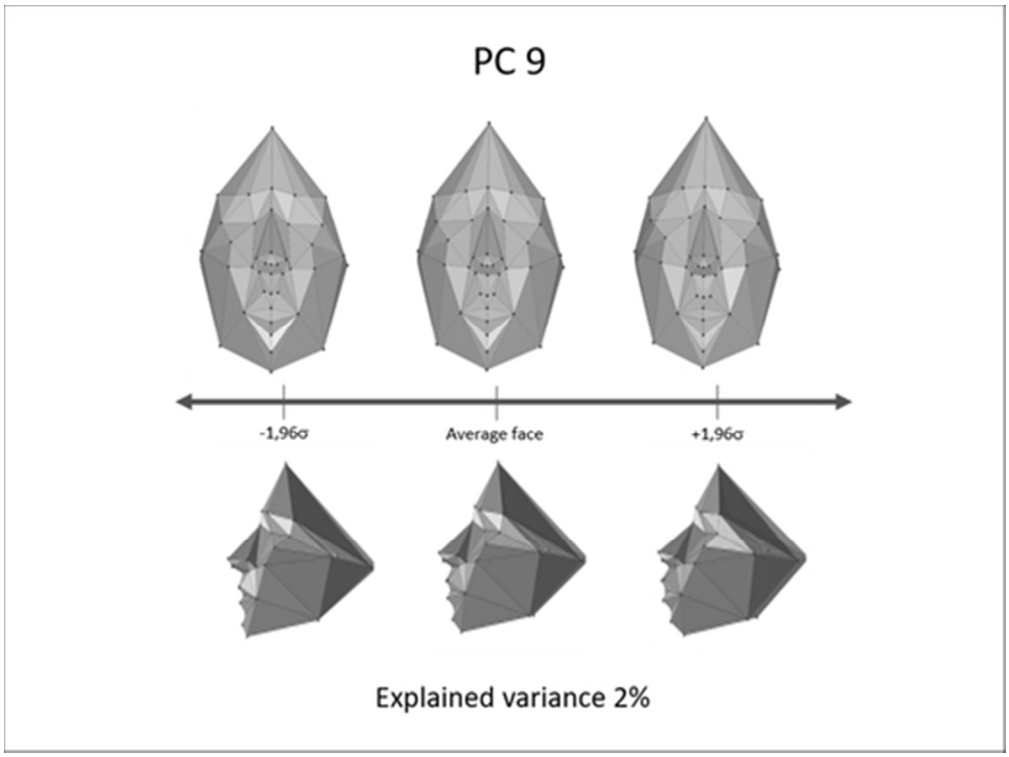

Effect of the variation of the three most significant PCs included in the regression model. For each PC, the average configuration, and those differing ± 1.96 SD, are depicted.

44x32mm (300 x 300 DPI)

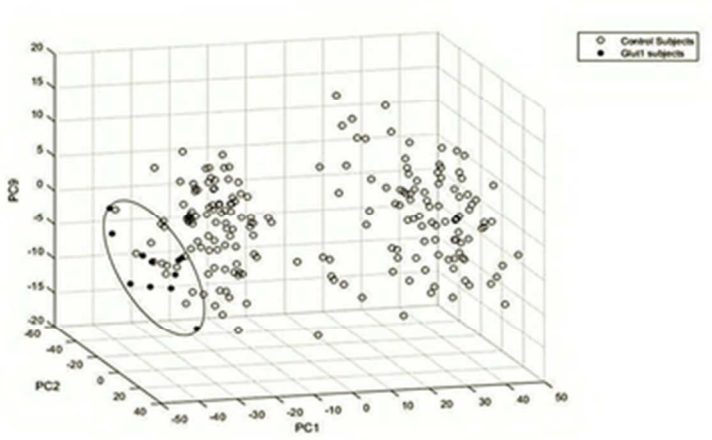

Comparison of Glut1-DS and control subjects in the principal component space, defined by the three more significant components included in the regression model. The ellipse highlights how the Glut1-DS subjects are distributed.

15x9mm (600 x 600 DPI)